Journal of The Electrochemical Society, **150** (10) A1333-A1338 (2003)
0013-4651/2003/150(10)/A1333/6/$7.00 © The Electrochemical Society, Inc.

Material Characterization and Electrochemical Performance of Hydrous Manganese Oxide Electrodes for Use in Electrochemical Pseudocapacitors

Jeng-Kuei Chang and Wen-Ta Tsai*,z

Department of Materials Science and Engineering, National Cheng Kung University, Tainan, Taiwan

Hydrous manganese oxide with promising pseudocapacitive behavior was deposited on a carbon substrate at anodic potentials of 0.5-0.95 V *vs.* saturated calomel electrode (SCE) in 0.25 M $Mn(CH_3COO)_2$ solution at 25°C. The effects of the deposition potential on the material characteristics and electrochemical performances of the hydrous manganese oxide prepared were investigated. Porous manganese oxide with higher crystallinity was formed at a lower deposition potential. When the deposition potential was 0.8 V_{SCE} or higher, the deposited oxide consisted of an inner layer with a laminated structure and a rough outer layer with nodules on the surface. X-ray photoelectron spectroscopy was also carried out to examine the chemical state of the deposited oxide. Analytical results indicated that the oxide was composed of both trivalent and tetravalent manganese oxides at a deposition potential of 0.5 V_{SCE}. However, the tetravalent manganese oxide became the dominant species in the film deposited at above 0.65 V_{SCE}. The manganese oxide formed at 0.5 V_{SCE} exhibited a specific capacitance as high as 240 F/g, as evaluated by cyclic voltammetry (CV) with a potential scan rate of 5 mV/s in 2 M KCl at 25°C. Increasing the CV scan rate reduced the specific capacitance. Only about 70% of the capacitance at 5 mV/s could be maintained when the CV scan rate was increased to 100 mV/s, for all the manganese oxide electrodes prepared. Moreover, a high deposition potential gave rise to a low specific capacitance of the manganese oxide formed.
 [DOI: 10.1149/1.1605744]

Manuscript submitted September 19, 2002; revised manuscript received April 22, 2003. Available electronically August 18, 2003.

Electrochemical capacitors (commonly referred to as supercapacitors) are charge-storage devices of high power and energy density, that exhibit excellent reversibility and a long cycle life.[1] Recently, they have become the subjects of increasing research interest due to their potential applications in several fields. These applications include loadleveling for batteries in electric vehicles during starting, acceleration, and regenerative braking,[2] as well as burst-power generation in electronic devices such as cellular phones, photodiode array, camcorders, and navigational devices among others. Accordingly, two kinds of electrochemical capacitors have been examined, the electric double layer capacitor and the electrochemical pseudocapacitor. The former typically consists of electrodes (for example, active carbon) with very high surface areas.[3,4] The nonfaradic separation of charges at the interface between a solid electrode and an electrolyte governs the capacitance of such a device.[5,6] On the other hand, the pseudocapacitance arises from fast, reversible faradic redox reactions that occur near an electrode surface over an appropriate range of potentials.[7-10] The difference between charge-storage mechanisms and the fact that carbon has been found to suffer from deterioration by oxidation and from high internal resistance[5] have caused the electrochemical pseudocapacitor to have attracted much attention for its potential supercapacitor applications.

Although amorphous hydrous ruthenium oxide prepared by the sol-gel process exhibits ideal pseudocapacitive behavior, a very large specific capacitance (over 700 F/g) and excellent reversibility,[7,8] the high cost of the material has limited its commercial use. Therefore, the search for a cheaper oxide with equivalent characteristics is attracting attention. The natural abundance of manganese oxide and its environmental compatibility make it a promising electrode material for use in various energy-storage technologies. Recently, several researchers have begun to develop an effective method for preparing manganese oxide with favorable pseudocapacitive characteristics. The preparations of powder manganese oxides by thermal decomposition[11] and coprecipitation[12] processes have been studied previously. The use of such oxide powders for fabricating electrodes (including: synthesize powder, mixing with a conducting agent and a binder, and making electrodes) is, however, complicated and inconvenient. A more effective preparation of manganese oxide electrodes for application in electrochemical capacitors is being sought. Hu and Tsou[13] reported that hydrous manganese oxide with ideal pseudocapacitive behavior could be prepared by anodic deposition in $MnSO_4$ on a carbon substrate. However, the physical and chemical nature of the oxide and the effects of the deposited conditions on the electrochemical characteristics of the oxide have not been well elucidated. Furthermore, the deposition rate in such media was low. So, anodic deposition of manganese oxide in other electrolytes at a high rate is of interest.

This investigation examined the deposition of manganese oxides on carbon substrate in 0.25 M manganese acetate solution at various anodic potentials (0.5-0.95 V *vs.* saturated calomel electrode, SCE). The properties of the deposited oxides are characterized by X-ray diffraction (XRD), scanning electron microscopy (SEM), confocal microscopy, and X-ray photoelectron spectroscopy (XPS). The electrochemical characteristics and pseudocapacitance of the manganese oxide deposited at various anodic potentials are also evaluated by cyclic voltammetry (CV).

Experimental

Manganese oxide was electroplated onto the $1 \times 1\ cm^2$ carbon substrates by anodic deposition in a neutral 0.25 M $Mn(CH_3COO)_2$ plating solution at 25°C. The substrates were first polished with SiC paper of grit 800, degreased with acetone and water, etched in a 25°C 0.2 M H_2SO_4 solution, and finally washed with pure water in an ultrasonic bath. During the deposition, the carbon substrate was held as the anode and a platinum sheet was used as the counter electrode. An SCE was used as the reference electrode. An EG&G Princeton Applied Research model 263 potentiostat was employed to control the deposited conditions. Anodic deposition was performed under constant applied potential. The applied potentials were varied in the range 0.5-0.95 V_{SCE} to give a total passed charge of 1.5 C. After electrodeposition, the electrode was dried in air. The amount of manganese oxide loaded onto the carbon substrate was then weighed using a microbalance with an accuracy of 10 μg.

The crystal structure of the manganese oxide deposited at various anodic potentials was determined by XRD. The patterns were recorded on a Rigaku D/MAX2500 diffractometer with a glancing-incident angle of 2°. The $K\alpha_1$ radiation of copper target with a wavelength of 1.54056 Å was used as the X-ray source. The detected diffraction angle (2θ) was scanned from 10° to 80° with a speed of 4° per min. The surface and cross-sectional morphologies of the prepared manganese oxides were observed using a scanning electron microscope (Philip XL-40FEG). The topography of the electrode

* Electrochemical Society Active Member.
z E-mail: wttsai@mail.ncku.edu.tw

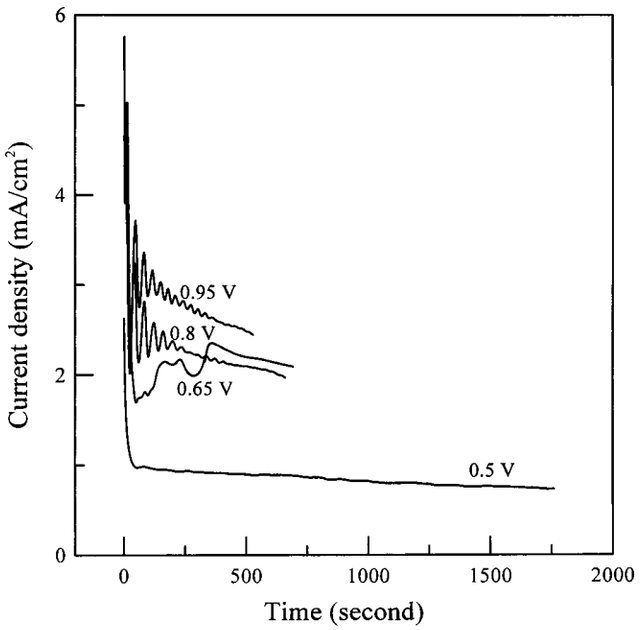

Figure 1. Variation of anodic current density of the electrodes formed at various deposition potentials in 0.25 M $Mn(CH_3COO)_2$ solution at 25°C.

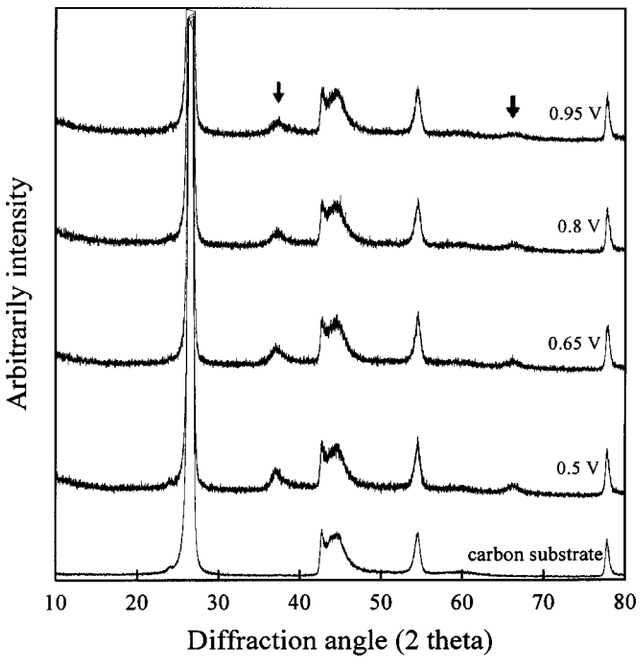

Figure 2. XRD patterns of the electrodes formed at various deposition potentials. Arrowed peaks were attributed to the oxides formed on the carbon substrates.

surface was further described via the confocal microscope (CM, Leica TCS SL). XPS was also carried out to evaluate the chemical state of the manganese oxide deposited at various anodic potentials. The measurements were performed with an ESCA 210 (VG Science Ltd.) spectrometer. Monochromated Al Kα (1486.6 eV) radiation was utilized as the X-ray source. The pressure in the analyzing chamber was approximately 1×10^{-9} Torr during the measurements.

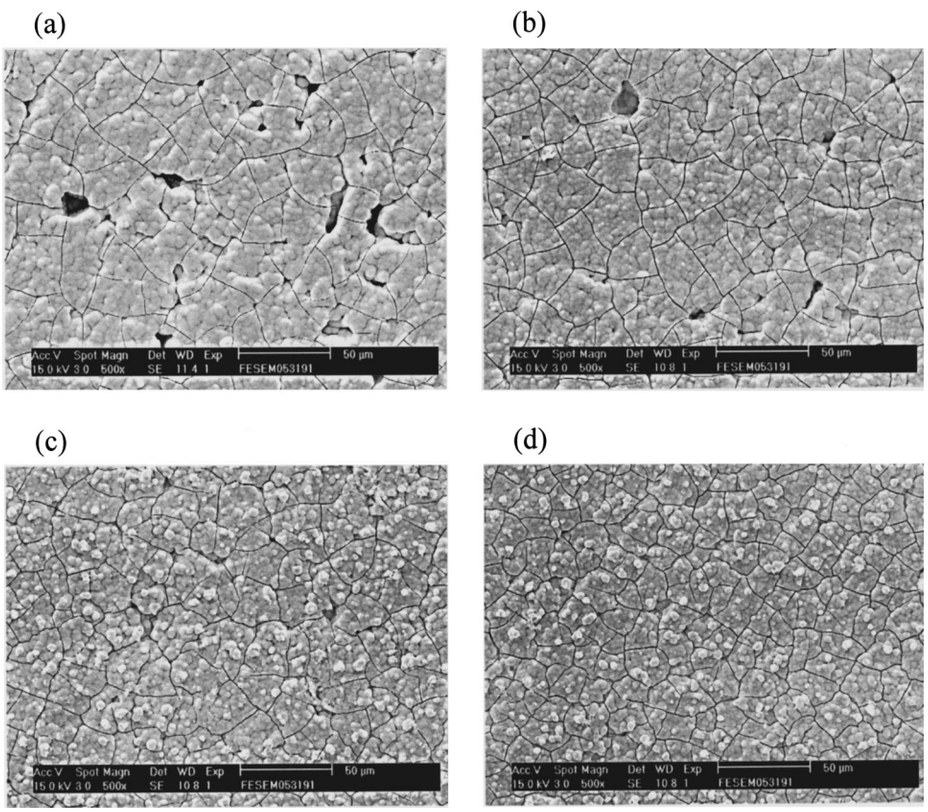

Figure 3. SEM micrographs showing the surfaces of the manganese oxides formed at various deposition potentials: (a) 0.5, (b) 0.65, (c) 0.8, and (d) 0.95 V_{SCE}.

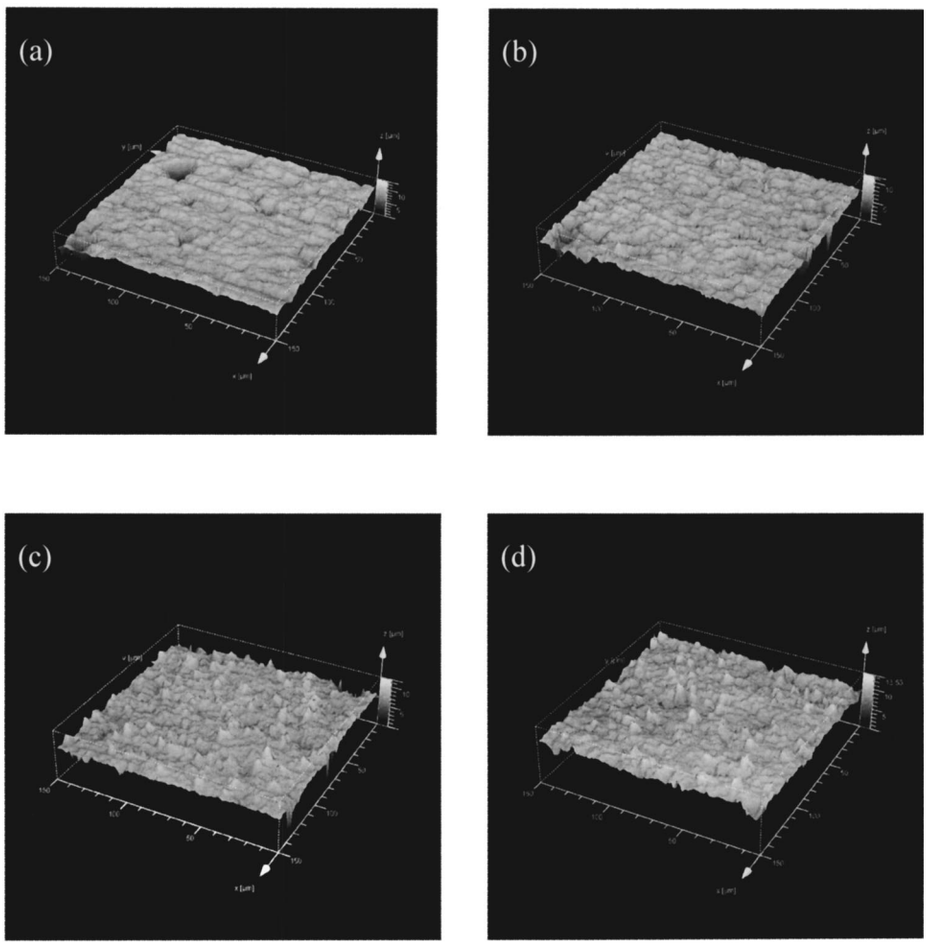

Figure 4. Surface topography of the manganese oxides formed at various deposition potentials of (a) 0.5, (b) 0.65, (c) 0.8, and (d) 0.95 V_{SCE} examined by the confocal microscope.

The electrochemistry of the manganese oxide was characterized by CV in 2 M KCl solution at room temperature. The test cell was a three-electrode system in which the manganese oxide electrode was assembled as the working electrode. A platinum sheet and an SCE were used as the counter electrode and the reference electrode, respectively. The measuring instrument was also an EG&G M263 potentiostat. The potential was cycled within a potential range of 0-1 V (*vs.* SCE). The CV scan rate was varied from 5 to 100 mV/s.

Results and Discussion

Anodic deposition of manganese oxide.—Figure 1 presents the variations of current densities during deposition in 0.25 M manganese acetate solution at 25°C and at various anodic potentials (0.5-0.95 V_{SCE}). Clearly, a higher applied anodic potential yielded a higher oxide deposition rate. For a total anodic pass charge of 1.5 C, 1760 s were required to deposit at an anodic potential of 0.5 V_{SCE}. When the potential was raised to 0.95 V_{SCE}, the required time was 530 s. The weight change of the electrodes before and after the deposition was measured by a microbalance. The amount of oxide deposited was in the range of 1.00-1.20 mg but seemed to increase gradually as anodic potential fell.

As can be seen in Fig. 1, an oscillation of the anodic current density occurred during anodic deposition, especially at higher potentials. It may be attributed to the exhaustion and resupply of the reactants near the electrode surface during deposition.

Material characterization.—XRD patterns revealed the crystalline structures of the manganese oxides deposited at various anodic potentials are demonstrated in Fig. 2. Besides the diffraction peaks associated with the carbon substrate, each pattern includes two peaks at 37.1° and 66.3° (marked by arrows). In the synthesis of manganese oxide from $KMnO_4$ solution, Jeong and Manthiram[14] also reported the existences of very weak and broad reflections at approximately 37° and 66° in the XRD patterns, suggesting that the oxide was nanocrystalline in nature. The broadening of the peaks at 37.1° and 66.3° as shown in Fig. 2, thus, indicates that the manganese oxide prepared had a nanocrystalline nature with poor crystallinity. The results shown in Fig. 2 also demonstrated that the peak intensity of the manganese oxides increased as the deposition potential decreased. The less broadened peaks, though not so obvious, for the manganese oxide formed at low deposition potential (say 0.5 V_{SCE}) suggested that a relatively higher crystallinity was obtained, perhaps because the deposition process was slower.

The surface morphologies of the manganese oxides deposited at various anodic potentials were examined by SEM. The micrographs shown in Fig. 3 clearly illustrate that the appearance of the oxide electrodes varied with the deposition potential. Cracks were observed on the surfaces of the deposited oxides and were caused by shrinkage stress during drying. At a lower anodic potential, the surface of the deposited manganese oxide contained some pores. As the potential was raised, the amount of pores declined and a relatively dense and compact surface was observed. A confocal microscope was also used to examine the surface contours of the electrodes on which were deposited with manganese oxide formed at various potentials. The results are shown in Fig. 4. At a potential of 0.5 V_{SCE}, holes with diam up to 20 μm were found on the surface. However, the surface was relatively smooth apart from the pore areas. The pore density decreased as the deposition potential was increased, consistent with the SEM micrographs shown in Fig. 3. At higher

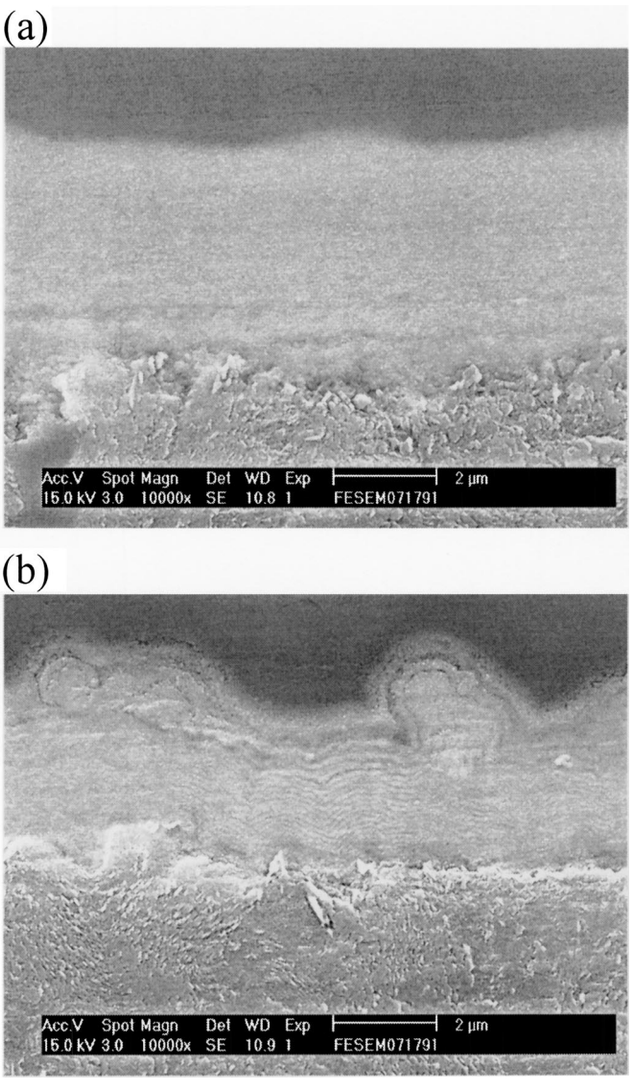

Figure 5. SEM micrographs showing the cross section of the manganese oxides formed at the deposition potentials of (a) 0.5 and (b) 0.8 V_{SCE} in 0.25 M $Mn(CH_3COO)_2$ solution at 25°C.

deposition potentials, 0.8 or 0.95 V_{SCE}, some small salients (approximately 3 μm high) were seen to stand on the surface of the electrodes such that the surface became rather rough.

SEM was used to further elucidate the cross section of the deposited manganese oxide. Figure 5 shows SEM micrographs of the surface oxide films formed at 0.5 and 0.8 V_{SCE}. As shown in Fig. 5a, manganese oxide with uniform thickness (about 5 μm) formed on the carbon substrate at 0.5 V_{SCE} was seen. The interface between the substrate and the deposited oxide was sound. When the deposition potential was raised to 0.8 V_{SCE}, a layered structure was observed. The thickness of the oxide layer was not uniform and the nodulous type of oxide appeared on top of the surface (Fig. 5b), indicating nonplanar growth of the oxide. The rough surface observed at high deposition potentials, as revealed in Fig. 3 and 4, was formed mainly due to the formation of nodulous oxide.

Closely examining the SEM micrograph shown in Fig. 5b reveals the layered structure of the oxide, particularly formed in the early stage. As demonstrated in Fig. 1, an oscillation in the current density during deposition process was observed. The depletion and replenishment of reactants at the electrode surface caused the fluctuation of current density, which subsequently resulted in the layered structure of the deposited oxide. Because the rate of consumption of reactant or formation of oxide was high at a high deposition potential, the supply of reactants to the reaction front became the rate-determining step in the later stage of oxide deposition. Under such conditions, the local fluctuation in the concentration of reactant would cause the nonplanar deposition of oxide, leading to the formation of oxide nodules, as depicted in Fig. 5b.

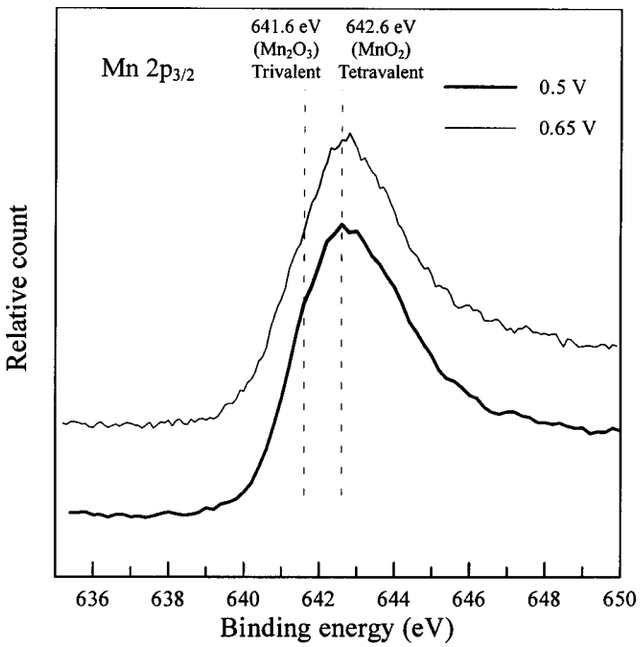

Figure 6. XPS spectra of the Mn $2p_{3/2}$ for the manganese oxides formed at the deposition potentials of (a) 0.5 and (b) 0.8 V_{SCE}.

Figure 6 presents the typical XPS spectra of the Mn $2p_{3/2}$ orbit of the manganese oxide deposited at anodic potentials of 0.5 and 0.65 V_{SCE}. Deconvolution of these spectra shows that both Mn^{3+} and Mn^{4+}, corresponding to 641.6 and 642.6 eV, respectively,[15,16] coexisted in the oxide formed at these two different potentials. In other words, the oxides were composed of both hydrated trivalent and tetravalent manganese oxide. However, the intensity of the spectrum that corresponded to Mn_2O_3 (641.6 eV) was reduced as the deposition potential was increased from 0.5 to 0.65 V_{SCE}, indicating that the amount of Mn_2O_3 in the oxide formed at a high potential was decreased. The analytic results revealed that tetravalent manganese oxide, instead of trivalent manganese oxide, was the dominant form of oxide deposited at the higher potentials.

Figure 7 shows the O 1s spectrum of the manganese oxide formed at 0.5 V_{SCE}. The binding energy of 531.8 eV corresponded to the water molecule (H-O-H), while that of 530.5 eV was associated with Mn-O-H hydroxide.[17] The fact that no peak corresponded to dehydrated manganese oxide in the O 1s spectrum reveals that the deposited oxide was mainly in hydrated form.

Electrochemical performance of the manganese oxide.—Figure 8 shows the cyclic voltammograms of the hydrous manganese oxides deposited at various anodic potentials measured in 2 M KCl solution at 25°C, with a potential scan rate of 20 mV/s. The open circuit potential of the deposited manganese oxides in 2 M KCl solution at 25°C were about 0.45-0.5 V_{SCE}. Within the potential range 0-1 V (*vs.* SCE), the oxide deposition potential slightly affected the voltammetric response of the manganese oxide. The voltammograms in Fig. 8 also reveal that the voltammetric current remained almost constant and exhibited the ideal capacitive characteristics. Although the shapes of the curves were similar, the specific voltammetric charge (voltammetric charge per gram of the deposited manganese

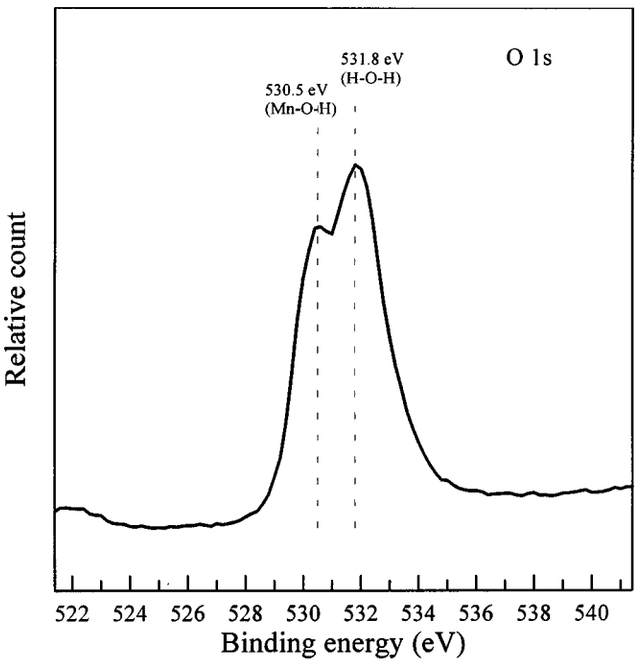

Figure 7. XPS spectra of the O 1s for the manganese oxides formed at the deposition potential of 0.5 V_{SCE}.

oxide), integrated from positive to negative sweeps decreased as deposition potential increased. The mean specific capacitance (C) of the manganese oxide could be estimated using the following equation.

$$C = \text{specific voltammetric charge/potential range} \quad [1]$$

Table I. Specific capacitance (F/g) of manganese oxides formed at various deposition potentials, measured in 2 M KCl solution at 25°C.

CV scan rate (mV/s)	Deposition potential (V_{SCE}) 0.5	0.65	0.8	0.95
5	240	223	209	191
10	201	191	183	168
20	189	178	170	156
40	179	168	161	146
60	171	162	154	140
80	166	157	149	135
100	163	152	144	130

The mean specific capacitances of the prepared manganese oxides, measured at a CV scan rate of 20 mV/s, were 189, 178, 170, and 156 F/g, respectively (as listed in Table I). Although a more amorphous structure and a rougher surface have been considered to be beneficial in increasing the specific capacitance of the oxide electrode for the supercapacitor,[8,18] the experimental results obtained in this investigation did not support this assertion. As mentioned above, the hydrous manganese oxide deposited at 0.5 V_{SCE} was composed of trivalent and tetravalent manganese oxides and more porous. The highest mean specific capacitance measured for the oxide deposited at 0.5 V_{SCE}, which had a relatively smooth surface and a high crystallinity, was probably attributable to the porous microstructure and the oxide's two different manganese oxidation states.

Effect of potential scan rate (10-100 mV/s) on the cyclic voltammetric behavior of the hydrous manganese oxide deposited at 0.65 V_{SCE} is demonstrated in Fig. 9. The curves were all roughly rectangular in shape and exhibited mirror-image characteristics that described capacitive behavior, even up to a potential scan rate of 100 mV/s. Similar results were obtained for other manganese oxide electrodes deposited at various potentials. All the cyclic voltammograms indicate that the high reversibility and excellent reactivity of the

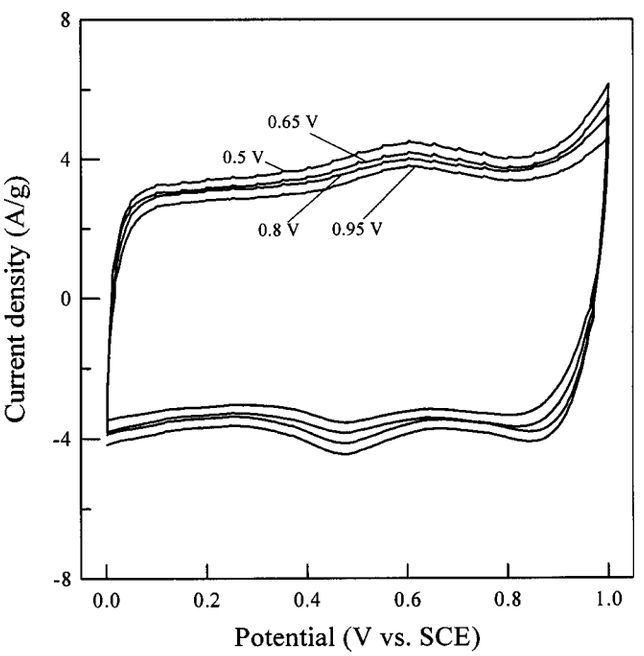

Figure 8. Cyclic voltammograms of the manganese oxides formed at various deposition potentials in 2 M KCl solution at 25°C with a potential scan rate of 20 mV/s.

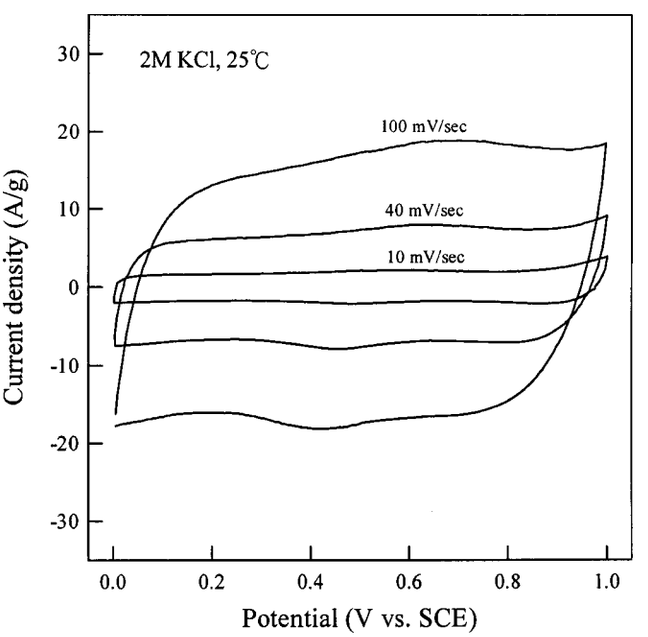

Figure 9. Effect of potential scanning rate on the voltammetric behavior of the manganese oxides formed at the deposition potentials of 0.65 V_{SCE} measured in 2 M KCl solution at 25°C.

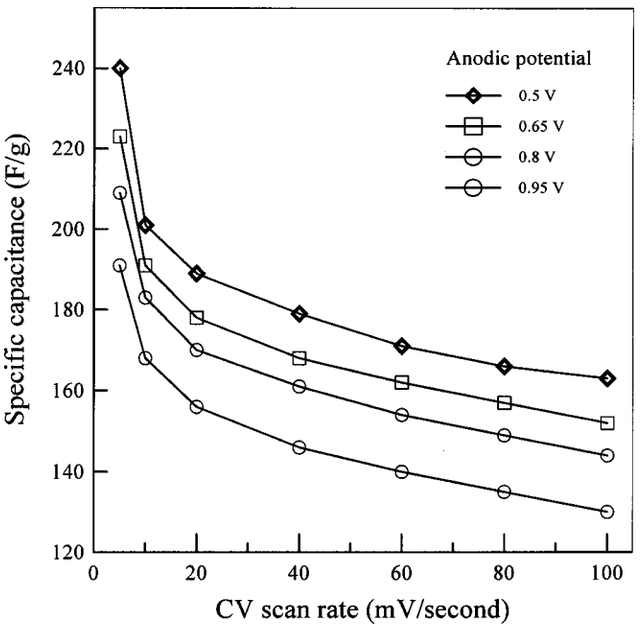

Figure 10. Effects of deposition potential and CV scan rate on the specific capacitance of the manganese oxide prepared.

hydrous manganese oxide prepared by anodic deposition in manganese acetate solution made it suitable for use in electrochemical capacitor (or supercapacitor) applications.

The effect of potential scan rate on the cyclic voltammetric measurement was also investigated in the range from 5 to 100 mV/s for all prepared manganese oxide electrodes. Table I summarizes the results. Clearly, the specific capacitances declined as the potential scan rate in CV increased for all the electrodes. As shown in Table I, the specific capacitance was decreased as the deposition potential was increased at any given potential scan rate. The highest obtained specific capacitance was 240 F/g for the manganese oxide electrode prepared at 0.5 V_{SCE} and evaluated at 5 mV/s in CV. The results are also plotted in Fig. 10, in which the dependences of deposition potential and CV scan rate are clearly demonstrated. When the scan rate was increased to 100 mV/s, the capacitance of the hydrous manganese oxide was reduced to about 70% of that measured at 5 mV/s regardless of the deposition potential.

Conclusions

Hydrous manganese oxide with promising pseudocapacitive behavior was successfully prepared on carbon substrate by anodic deposition (0.5-0.95 V_{SCE}) in 0.25 M manganese acetate solution at 25°C. The material characteristics and electrochemical performance of the manganese oxides were shown to depend on the deposition potential. At a lower deposition potential, porous manganese oxide with a higher crystallinity was formed. When the deposition potential was 0.8 V_{SCE} or higher, the deposited oxide consisted of an inner layer with a laminated structure and a rough outer layer with nodules on the surface. At a deposition potential of 0.5 V_{SCE}, the oxide was composed of both trivalent and tetravalent manganese oxides. When the deposition potential was raised above 0.65 V_{SCE}, the amount of trivalent manganese oxide was diminished while the tetravalent manganese oxide became the dominant species in the deposited film. The results of cyclic voltammetry showed that a specific capacitance of 240 F/g could be obtained for the manganese oxide formed at 0.5 V_{SCE} in 2 M KCl solution, at a potential scan rate of 5 mV/s. The specific capacitance declined as the deposited oxide became less porous and the amount of trivalent manganese oxide was diminished. Furthermore, the specific capacitance evaluated by CV decreased as the potential scan rate increased. Only about 70% of the capacitance obtained at 5 mV/s could be maintained when the scan rate was increased to 100 mV/s.

Acknowledgments

The authors would like to thank the National Science Council of the Republic of China for financially supporting this research under contract no. NSC 90-2216-E-006-070.

National Cheng Kung University assisted in meeting the publication costs of this article.

References

1. B. E. Conway, *Electrochemical Supercapacitors*, Kluwer-Plenum, New York (1999).
2. A. F. Burke and T. C. Murphy, *Mater. Res. Soc. Symp. Proc.*, **393**, 375 (1995).
3. M. Ishikawa, M. Morita, M. Ihara, and Y. Matsuda, *J. Electrochem. Soc.*, **141**, 1730 (1994).
4. B. Pillay and J. Newman, *J. Electrochem. Soc.*, **143**, 1806 (1996).
5. S. Sarangapani, B. V. Tilak, and C. P. Chen, *J. Electrochem. Soc.*, **143**, 3791 (1996).
6. S. Sarangapani, P. Lessner, J. Forchione, A. Griffith, and A. B. Laconti, *J. Power Sources*, **29**, 355 (1990).
7. J. P. Zheng and T. R. Jow, *J. Electrochem. Soc.*, **142**, L6 (1995).
8. J. P. Zheng, P. J. Cygan, and T. R. Jow, *J. Electrochem. Soc.*, **142**, 2699 (1995).
9. B. E. Conway, *J. Electrochem. Soc.*, **138**, 1539 (1991).
10. Y. Takasu, T. Nakamura, H. Ohkawauchi, and Y. Murakami, *J. Electrochem. Soc.*, **144**, 2601 (1997).
11. H. Y. Lee, V. Manivannan, and J. B. Goodenough, *Comptes Rendus Chimie*, **2**, 565 (1999).
12. H. Y. Lee and J. B. Goodenough, *J. Solid State Chem.*, **144**, 220 (1999).
13. C. C. Hu and T. W. Tsou, *Electrochem. Commun.*, **4**, 105 (2002).
14. Y. U. Jeong and A. Manthriram, *J. Electrochem. Soc.*, **149**, A1419 (2002).
15. B. R. Strohmeier and D. M. Hercules, *J. Phys. Chem.*, **88**, 4922 (1984).
16. B. N. Ivanov-Emin, N. A. Nevskaya, B. E. Zaitsev, T. M. Ivanova, *Zh. Neorg. Khim.*, **27**, 3101 (1982).
17. M. Chigane and M. Ishikawa, *J. Electrochem. Soc.*, **147**, 2246 (2000).
18. J. P. Zheng, T. R. Jow, Q. X. Jia, and X. D. Wu, *J. Electrochem. Soc.*, **143**, 1068 (1996).